# BASIC AND TRANSLATIONAL—ALIMENTARY TRACT

## Card9 Mediates Intestinal Epithelial Cell Restitution, T-Helper 17 Responses, and Control of Bacterial Infection in Mice

HARRY SOKOL,[1,2,3,*] KARA L. CONWAY,[1,2,4,*] MEI ZHANG,[5] MYUNGHWAN CHOI,[6] BRET MORIN,[1,2,4] ZHIFANG CAO,[1,2] EDUARDO J. VILLABLANCA,[1,2] CHUN LI,[1,2] CISCA WIJMENGA,[7] SEOK HYUN YUN,[6] HAI NING SHI,[5] and RAMNIK J. XAVIER[1,2,4]

[1]*Gastrointestinal Unit and Center for the Study of Inflammatory Bowel Disease,* [2]*Center for Computational and Integrative Biology,* [6]*Wellman Center for Photomedicine, Massachusetts General Hospital, Harvard Medical School, Boston, Massachusetts;* [3]*Gastroenterology Department, Saint Antoine Hospital, Assistance Publique Hôpitaux de Paris, Paris, France;* [4]*Broad Institute of Massachusetts Institute of Technology and Harvard University, Cambridge, Massachusetts;* [5]*Mucosal Immunology Laboratory, Massachusetts General Hospital, Harvard Medical School, Charlestown, Massachusetts;* [7]*University of Groningen, University Medical Center Groningen, Department of Genetics, Groningen, The Netherlands*

**BACKGROUND & AIMS:** Caspase recruitment domain 9 (CARD9) is an adaptor protein that integrates signals downstream of pattern recognition receptors. CARD9 has been associated with autoinflammatory disorders, and loss-of-function mutations have been associated with chronic mucocutaneous candidiasis, but the role of CARD9 in intestinal inflammation is unknown. We characterized the role of Card9 in mucosal immune responses to intestinal epithelial injury and infection. **METHODS:** We induced intestinal inflammation in Card9-null mice by administration of dextran sulfate sodium (DSS) or *Citrobacter rodentium*. We analyzed body weight, assessed inflammation by histology, and measured levels of cytokines and chemokines using quantitative reverse-transcription polymerase chain reaction and enzyme-linked immunosorbent assay. Cell populations were compared between wild-type and Card9-null mice by flow cytometry analysis. **RESULTS:** Colon tissues and mesenteric lymph nodes of Card9-null mice had reduced levels of interleukin (IL)-6, interferon-γ, and T-helper (Th)17 cytokines after administration of DSS, compared with wild-type mice. IL-17A and IL-22 expression were reduced in the recovery phase after DSS administration, coincident with decreased expression of antimicrobial peptides and the chemokine (C-C motif) ligand 20 (Ccl20). Although Card9-null mice had more intestinal fungi based on 18S analysis, their Th17 responses remained defective even when an antifungal agent was administered throughout DSS exposure. Moreover, Card9-null mice had impaired immune responses to *C rodentium*, characterized by decreased levels of colonic IL-6, IL-17A, IL-22, and regenerating islet-derived 3 gamma (RegIIIγ), as well as fewer IL-22–producing innate lymphoid cells (ILCs) in colon lamina propria. **CONCLUSIONS: The adaptor protein CARD9 coordinates Th17- and innate lymphoid cell–mediated intestinal immune responses after epithelial injury in mice.**

*Keywords:* Colitis; ILC; Inflammatory Response; Mouse Model.

The gastrointestinal tract is lined by epithelium, which not only serves as a protective barrier but also assists in nutrient absorption and innate immunity. The mucosa exists in dynamic equilibrium with luminal flora and dietary antigens, and immune homeostasis is maintained with the aid of a pre-epithelial layer consisting of protective mucus, antimicrobial peptides (AMPs), and IgA. The intestinal immune system is poised to detect bacterial antigens at the mucosal surface and drive appropriate responses, depending on the nature of the stimulus, to maintain tolerance or initiate immune signaling. In some circumstances, tolerance toward the microbiota is lost, leading to inappropriate immune responses and inflammation. This is the case in inflammatory bowel diseases such as Crohn's disease and ulcerative colitis, and, importantly, an altered composition of the gut microbiota, termed *dysbiosis*, has been reported in inflammatory bowel disease patients.

Caspase recruitment domain 9 (CARD9) is an adaptor protein that assists in the integration of signals downstream of pattern recognition receptors.[1] In particular, CARD9 plays a major role in sensing fungi via several C-type lectins including dectin-1, dectin-2, and mincle. For example, dectin-1 binding by β-glucan, a component of the fungal wall, successively induces the activation of SYK, CARD9, Bcl10, and MALT1, leading to activation of nuclear factor-κB, c-Jun-N-terminal kinase (JNK), and p38

[*] Authors share co-first authorship.

*Abbreviations used in this paper:* AMP, antimicrobial peptide; ASCA, anti–*Saccharomyces cerevisiae* antibody; CARD9, caspase recruitment domain 9; Ccl20, chemokine (C-C motif) ligand 20; CFU, colony forming unit; DSS, dextran sulfate sodium; IFN, interferon; IL, interleukin; ILC, innate lymphoid cell; JNK, c-Jun-N-terminal kinase; LP, lamina propria; MLN, mesenteric lymph node; PBS, phosphate-buffered saline; qRT-PCR, quantitative reverse-transcription polymerase chain reaction; SFB, segmented filamentous bacteria; Th, T-helper; TNF, tumor necrosis factor.

© 2013 by the AGA Institute
0016-5085/$36.00
http://dx.doi.org/10.1053/j.gastro.2013.05.047

mitogen-activated protein kinase pathways.[2,3] Furthermore, CARD9 is required to mount adaptive T-helper (Th)17 responses during fungal infection via dectin-1[4–6] and during *Mycobacteria* infection via mincle.[7] A loss-of-function mutation in *CARD9* was identified in patients with chronic mucocutaneous candidiasis and congenital susceptibility to *Candida*,[4] supporting a role for CARD9 in antifungal innate immunity in human beings.

In addition to its role in sensing fungi, CARD9 is involved in innate immune responses to bacteria and viruses. CARD9 mediates mincle-dependent *Mycobacteria* sensing and Nod2-dependent p38/JNK signaling,[8] enhances Toll-like receptor signaling,[9,10] and facilitates microbe-elicited reactive oxygen species production.[11] Furthermore, p38 and JNK activation, as well as cytokine production after infection with RNA viruses, relies on CARD9 through Mda5, RIG-I, and MAVS.[12] CARD9 is therefore a key adapter protein for innate immunity against a range of microorganisms including intestinal commensals and pathogens.

Although the role of CARD9 in systemic immunity has been explored,[1] its function in the gastrointestinal immune system has not yet been investigated. Here, we show that Card9 is a key molecule in intestinal homeostasis and is required to mount appropriate interleukin (IL)-6, IL-17A, interferon (IFN)γ, and IL-22 responses. We show that Card9-null mice are more susceptible to dextran sulfate sodium (DSS)-induced colitis and that recovery is impaired in this model. The enhanced inflammation in Card9-null mice is characterized by defective IFNγ and Th17 cytokine responses, as well as impaired chemokine responses. By using the Th17-dependent *Citrobacter rodentium* colitis model, we further show that Card9-null mice have fewer colonic Th17 cells and innate lymphoid cells (ILCs) than wild-type mice. As a result, Card9-null mice develop more severe inflammation during *C rodentium*–induced colitis, indicating that Card9 is important to reestablish homeostasis after epithelial injury.



## Materials and Methods

### DSS

Mice were fed 3% (wt/vol) DSS (molecular weight, 36,000–50,000; MP Biomedicals, Solon, OH) dissolved in sterile drinking water ad libitum. Animals were monitored daily for weight loss.

### C rodentium *Infection*

Mice were inoculated orally with *C rodentium* (strain DBS100; American Type Culture Collection, Manassas, VA) as previously described.[13,14] Bacteria were grown overnight in Luria broth and resuspended in phosphate-buffered saline (PBS) before infection (0.5 mL/mouse, $1 \times 10^9$ colony forming units [CFU] unless otherwise noted). When used, nalidixic acid was administered by intragastric gavage (100 mg/mice) 24 hours before infection with *C rodentium*. To assess clearance of *C rodentium*, fecal pellets were homogenized, serially diluted, and plated onto selective MacConkey agar (selective for gram-negative organisms). After overnight culture at 37°C, colonies were counted based on the size and distinctive appearance of *C rodentium* colonies (pink center with white outer rim), as described previously.

### *Lymphocyte Isolation and Measurement of Cytokine Production*

Lymphocytes were cultured in the presence or absence of anti-CD3 (10 μg/mL) or *C rodentium* Antigen (50 μg/mL) for 72 hours. Supernatants were analyzed using an enzyme-linked immunosorbent assay (see the Supplementary Materials and Methods section for details).

### *Ccl20 Assay*

Splenic macrophages were isolated using MACs CD11b$^+$ magnetic beads per the manufacturer's protocol (Miltenyi Biotec, Auburn, CA). Cells ($1 \times 10^5$) were stimulated with 100 ng/mL lipopolysaccharide, 10 μg/mL muramyl dipeptide, and 50 μg/mL tumor necrosis factor (TNF)-α for 4 days, and supernatants were analyzed for chemokine (C-C motif) ligand 20 (Ccl20) production per the manufacturer's protocol (Quantikine; R&D Systems, Minneapolis, MN).

### *Laser Injury and Epithelial Permeability Assay*

We used a custom-built, 2-photon endomicroscopy system with a side-view probe as previously described.[15,16] Microwounds were introduced in colonic epithelium via laser, and the epithelial barrier function was assessed 4 days later (see the Supplementary Materials and Methods section for details).

### *Fungal Translocation*

Mesenteric lymph nodes (MLNs) were harvested after DSS recovery (day 12) and 18S ribosomal RNA levels were determined using quantitative reverse-transcription polymerase chain reaction (qRT-PCR) normalized to glyceraldehyde-3-phosphate dehydrogenase (see the Supplementary Materials and Methods section for details).

### *Mouse Anti-*Saccharomyces cerevisiae *Antibody Detection*

Serum was harvested on days 0, 7, and 12 after DSS exposure as described earlier. Anti–*Saccharomyces cerevisiae* antibody (ASCA) levels were quantified by an enzyme-linked immunosorbent assay (MyBiosource, San Diego, CA).

### *Fluconazole Administration*

Mice were fed 0.5 mg/mL fluconazole in drinking water (Sigma-Aldrich, St. Louis, MO) 2 days before DSS administration, and everyday thereafter, as previously described.[17]

### *Lamina Propria Isolation*

Colonic and small intestine lamina propria (LP) cells were isolated as previously described with slight modifications (see the Supplementary Materials and Methods section for details).

### *Statistics*

Statistical analyses were performed using the 2-tailed Student *t* test for unpaired data or by the nonparametric Mann–Whitney test. Differences with a *P* value less than .05 were considered significant.

## Results

### *Card9-Null Mice Show Impaired Recovery After DSS-Induced Injury*

To determine the role of Card9 in mucosal immune responses, we worked with 2 mouse models of epithelial injury. Previous studies have shown that Card9-null mice have normal B-cell, T-cell, and myeloid cell development and function, suggesting that the immune system is intact.[1] Upon histologic examination, intestinal epithelial cell distribution appeared normal, including Paneth and goblet cells, and we did not observe spontaneous colitis (data not shown). We therefore decided to induce intestinal injury and inflammation using the DSS colitis model. Mice were killed after receiving 3% DSS in their drinking water for 7 days (acute injury, day 7), or after an additional 5 days in which DSS was discontinued (recovery, day 12). The severity of acute injury (defined by weight loss, colon length, and histologic score) was not statistically different between wild-type and Card9-null mice 7 days after initial DSS exposure (Supplementary Figure 1). However, during recovery, Card9-null mice had greater body weight loss (Figure 1*A*). Colon shortening, a macroscopic parameter of colitis severity, was more pronounced in Card9-null mice than in wild-type littermates (5.68 ± 0.23 cm vs 6.99 ± 0.30 cm; Figure 1*B*), and histologic scores were significantly higher in Card9-null mice (Figure 1*C* and *D*) 5 days after DSS was discontinued. These deficits during the recovery phase after DSS injury suggest that Card9 may play a role in intestinal healing.

### *Card9-Null Mice Show Impaired Immune Responses After DSS Administration*

To decipher the mechanisms leading to defective recovery from DSS-induced injury in Card9-null mice, we assessed colonic expression levels of both proinflammatory cytokines and cytokines that promote epithelial healing via qRT-PCR (Figure 2*A*). No significant differences were observed between wild-type and Card9-null mice in the absence of DSS (data not shown). We observed that during acute injury and after discontinuing DSS (recovery), the expression of TNF$\alpha$, IL-10, and IL-23R were increased similarly in wild-type and Card9-null mice, whereas IL-23, IL-17A, and IFN$\gamma$ were significantly lower in Card9-null mice. The expression of IL-6, IL-17F, IL-21, and IL-22 also were decreased significantly in Card9-null colon compared with wild-type, however, only during recovery after DSS was discontinued (Figure 2*A*). Systemic IL-6 and IL-17A were similar in wild-type and Card9-null mice after recovery, suggesting that these responses were specific for the intestinal environment (Supplementary Figure 2*A*). Furthermore, we found decreased IFN$\gamma$, IL-17A, IL-21, and IL-22 expression in Card9-null MLNs compared with wild-type, as well as impaired IFN$\gamma$ and IL-17A secretion after T-cell stimulation (Figure 2*B*). These results suggest that deficient IL-17 and IL-22 cytokine responses may underlie the defective recovery of Card9-null mice during DSS-induced epithelial injury. Importantly, IL-6 protects the intestinal epithelium from injury by regulating intestinal trefoil factor and/or AMP secretion.[18,19] Therefore, the defect in IL-6 expression observed in Card9-null mice also may play a role in impaired epithelial restitution.

Chemokines play a major role in recruiting immune cells to sites of injury or infection. Ccl20 is involved in recruitment of Ccr6-expressing cells, including Th17 cells and ILCs, which are the main producers of IL-17 and IL-22

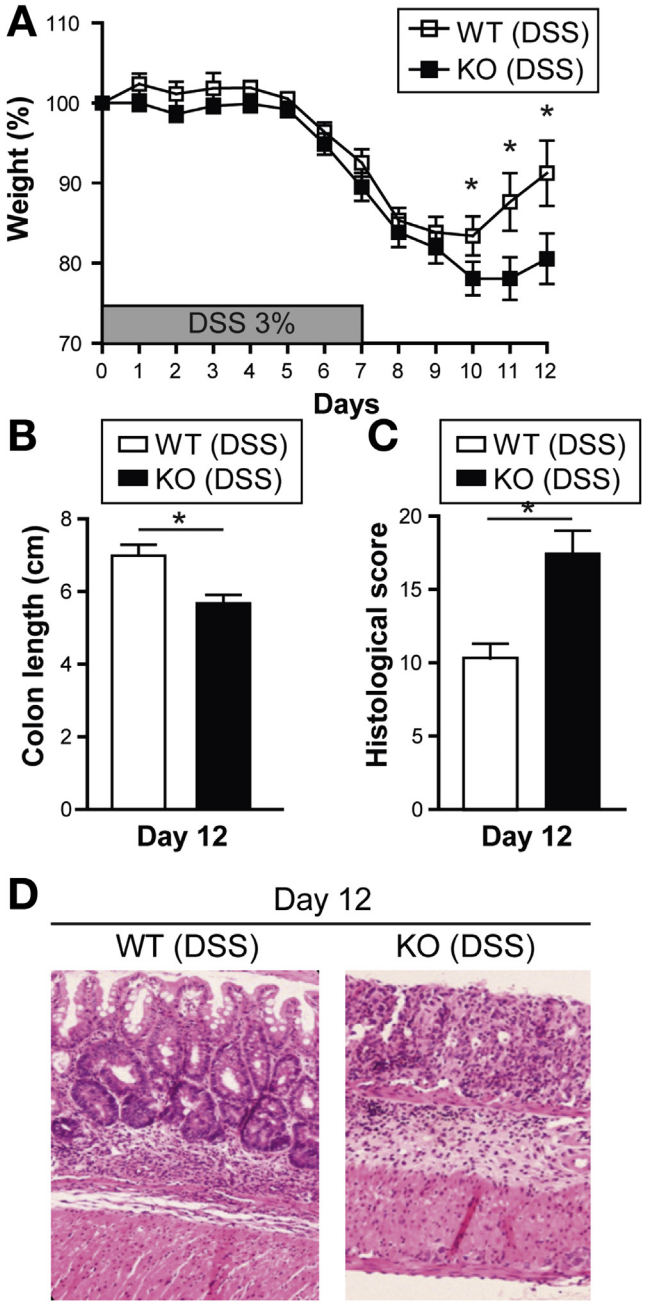


**Figure 1.** Card9-null mice show impaired recovery after DSS-induced injury. (*A*) Weight loss in DSS-exposed wild-type (WT) and Card9-null (KO) mice. (*B*) Colon length of WT and KO mice after administration of DSS. (*C*) Histologic score of WT and KO mice after administration of DSS. (*D*) H&E staining of representative cross-sections of medial colon (magnification, 20×). Data are representative of at least 2 independent experiments (N = 5). Error bars represent SEM. *$P < .05$.

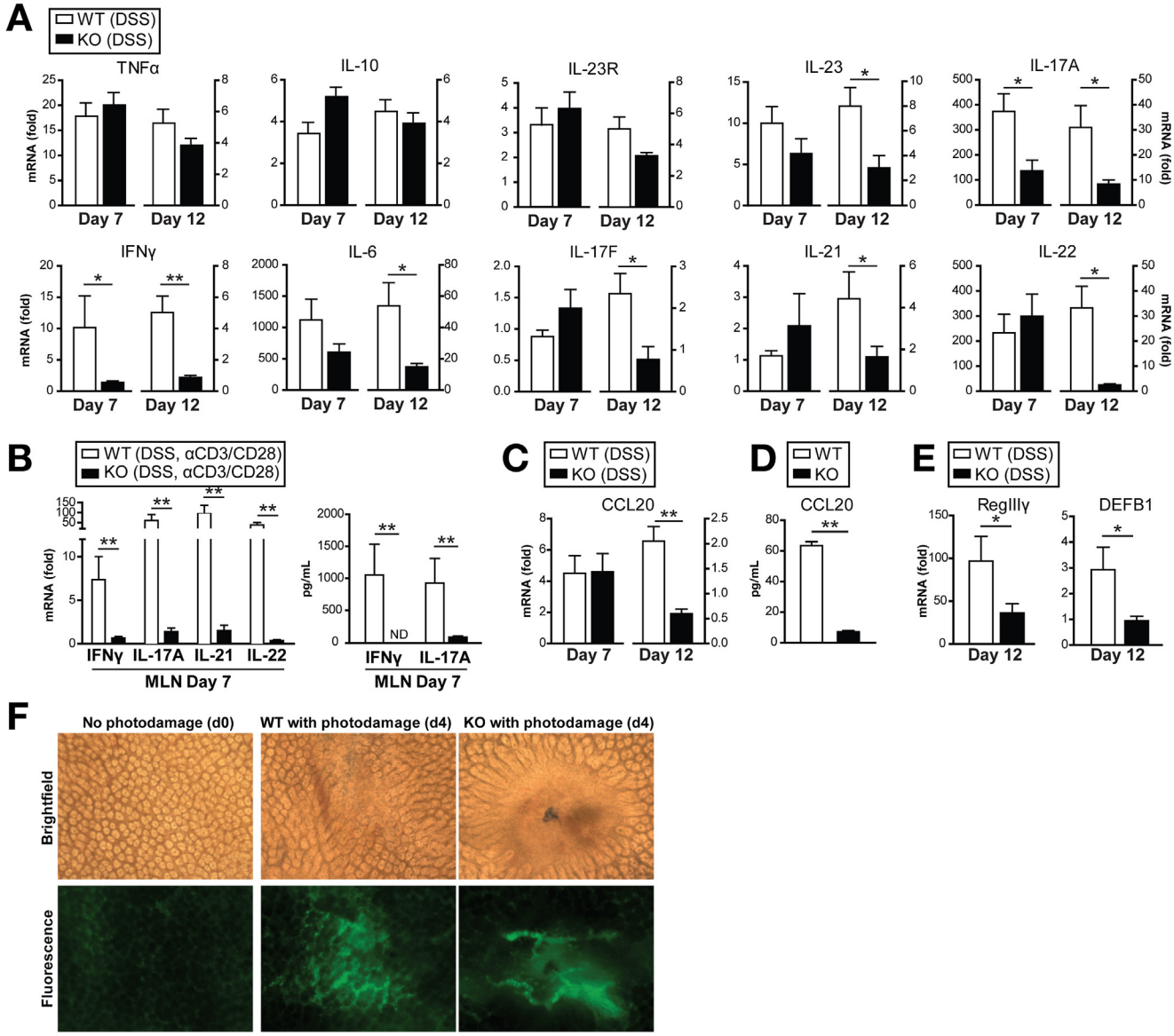


**Figure 2.** Card9-null mice show impaired immune responses after DSS administration. (*A*) Cytokine expression in colon of wild-type (WT) and Card9-null (KO) mice as quantified by qRT-PCR. Data are shown as fold changes relative to WT mice without DSS for each time point. (*B*) Cytokine expression by qRT-PCR (*left*) and secretion by ELISA (*right*) in MLN cells after DSS administration and after stimulation with anti-CD3/anti-CD28 antibodies. Data are shown as fold changes relative to WT mice without anti-CD3/anti-CD28. (*C*) Ccl20 expression in colon of WT and KO mice after DSS administration. Quantification by qRT-PCR. Data are shown as fold changes relative to WT mice without DSS for each time point. (*D*) Isolated splenic macrophages were stimulated with 100 ng/mL lipopolysaccharide, 10 $\mu$g/mL MDP, and 50 $\mu$g/mL TNF$\alpha$ for 4 days. Culture supernatants were harvested and analyzed for Ccl20 via enzyme-linked immunosorbent assay. (*E*) AMP expression in colon of WT and KO mice after recovery from DSS-induced injury. Quantification by qRT-PCR. Data are shown as fold changes relative to WT mice without DSS. (*F*) Femtosecond laser injuries were introduced into colonic epithelium via a 2-photon endomicroscopy system. Mice were injected with 2 million Daltons fluorescein isothiocyanate dextran before colonoscopy to determine successful photodamage (formation of intravascular clots and extravasation of fluorescent dye after laser exposure). Four days after injury, colons were stained with Evans Blue dye and imaged using bright-field microscopy (*top*). Residual fluorescein isothiocyanate fluorescence also was assessed using fluorescence microscopy (*bottom*). Data are representative of at least 2 independent experiments (N = 5). Error bars represent SEM. $^{*}P < .05$, $^{**}P < .01$. ND, not detectable.

in the gut. In agreement with the cytokine expression results, which showed lower levels of IL-17A, IL-21, and IL-22 in Card9-null colon, expression of the chemokines Ccl20 and monocyte chemoattractant protein-1 (Mcp1) were decreased significantly in Card9-null colon, compared with wild-type, 5 days after DSS was discontinued (Figure 2*C* and Supplementary Figure 2*B*). Moreover, when primary macrophages, key Ccl20 secretors, were activated ex vivo, Card9-null macrophages showed impaired production of the Th17-recruiting chemokine (Figure 2*D*).

To investigate the consequences of reduced IL-17 and IL-22 expression in the intestine of Card9-null mice, we assessed downstream effectors induced by these cytokines. IL-22–mediated signaling acts through STAT3 to regulate mucosal wound healing in intestinal epithelial cells.[20]

BASIC AND TRANSLATIONAL AT

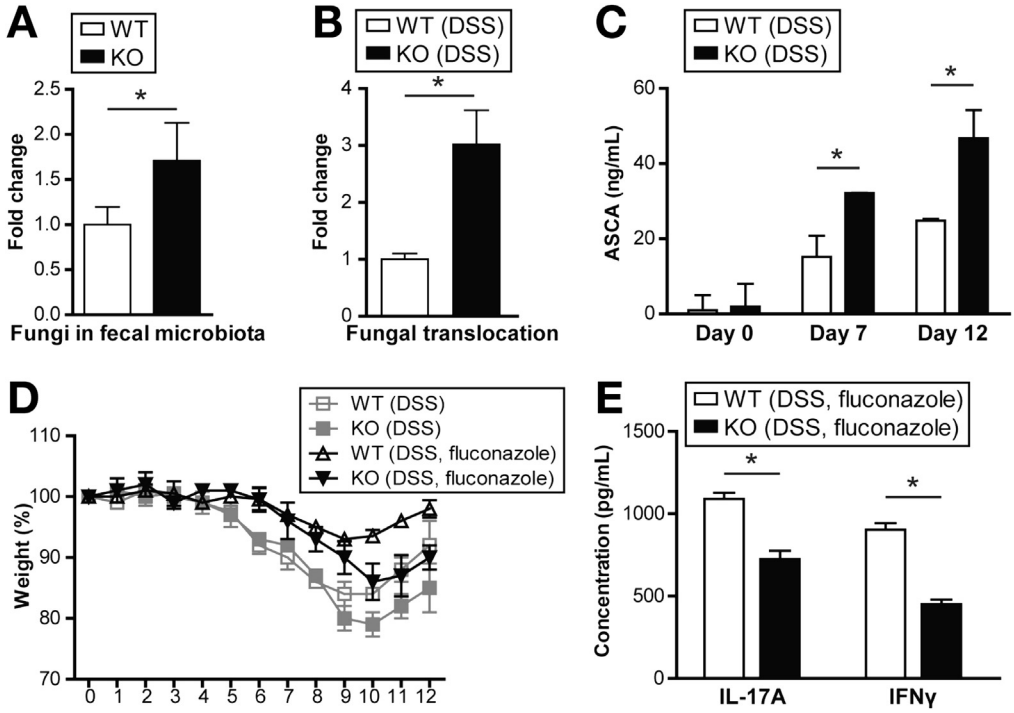


**Figure 3.** Card9 is required to control fungi in gut microbiota. (*A*) Basal fungi levels in fecal microbiota of wild-type (WT) and Card9-null (KO) mice were quantified by 18S qRT-PCR, normalized to the threshold cycle value of the 16S ribosomal RNA gene. Data are plotted relative to WT mice. (*B*) MLNs were harvested 5 days after DSS was discontinued, and 18S fungi levels were determined by qRT-PCR normalized to glyceraldehyde-3-phosphate dehydrogenase. Data are plotted relative to WT mice. (*C*) Serum ASCA concentrations were quantified on days 0, 7 (acute injury), and 12 (recovery) via enzyme-linked immunosorbent assay. (*D*) Weight loss in DSS-treated WT and KO mice. Indicated mice were treated with 0.5 mg/mL fluconazole 2 days before, and throughout the 12-day DSS course described earlier. (*E*) MLN T cells from fluconazole-treated mice (after acute injury) were stimulated with anti-CD3/anti-CD28 for detection of IFNγ and IL-17A by enzyme-linked immunosorbent assay. Data are representative of at least 2 independent experiments (N = 5–6). Error bars represent SEM. *$P < .05$.



Similar to Card9-null mice, IL-22-null mice develop more severe DSS-induced colitis as measured by weight loss and disease activity, with major differences during recovery.[20] IL-22 induces expression of AMPs and the antibacterial protein regenerating islet-derived 3 gamma (RegIIIγ) in epithelial cells.[21] In line with these data, the expression of RegIIIγ in Card9-null colon was significantly lower than in wild-type mice 5 days after DSS was discontinued (Figure 2*E*). Moreover, in accordance with the role of IL-17A and IL-17F in the induction of colonic β-defensin (DEFB1) expression,[22] β-defensin 1 expression was decreased in Card9-null colon, compared with wild-type, after 5 days of recovery (Figure 2*E*). Decreased AMP expression in Card9-null mice after recovery may lead to altered responses to intestinal microbiota and suggests one potential mechanism for the observed restitution defect.

To directly assess the defective epithelial restitution in Card9-null mice, we used an in vivo model system to induce epithelial microwounds using laser photodamage. By using 2-photon endomicroscopy, we were able to induce photodamage in the colonic epithelium of wild-type and Card9-null mice and assess epithelial permeability over time. After 4 days, Card9-null epithelium showed more vascular leakage (as detected via fluorescein isothiocyanate dextran) and epithelial permeability (as detected by Evans Blue dye) at the site of injury (Figure 2*F*). Moreover, although the site of injury was not detected in wild-type mice after 7 days, the site of injury remained identifiable in Card9-null mice at this time point, indicating impaired wound healing (data not shown). Thus, Card9 regulates wound healing, possibly via IL-22-specific functions.

Taken together, these results show that, after DSS exposure, Card9-null mice show impaired epithelial recovery, which is characterized by defective Th17 cytokines, IFNγ, and IL-6 production. The data suggest that repair processes are compromised, which can be explained in part by defective production of restitutive cytokines and AMPs.

### *Card9 Is Required to Control Fungi in Gut Microbiota*

Given the impaired Th17 responses observed in Card9-null mice after DSS injury, we next quantified the level of segmented filamentous bacteria (SFB) present in wild-type and Card9-null mice, because SFB colonization is required for Th17 cell development[23,24] (Supplementary Figure 3). We found no difference in SFB levels between wild-type and Card9-null mice in the gut microbiota, ruling out a role for defective SFB colonization in the Th17 phenotype observed in Card9-null mice.

Because Card9 is involved in the immune response to fungi, we also assessed the level of total fungi in the gut

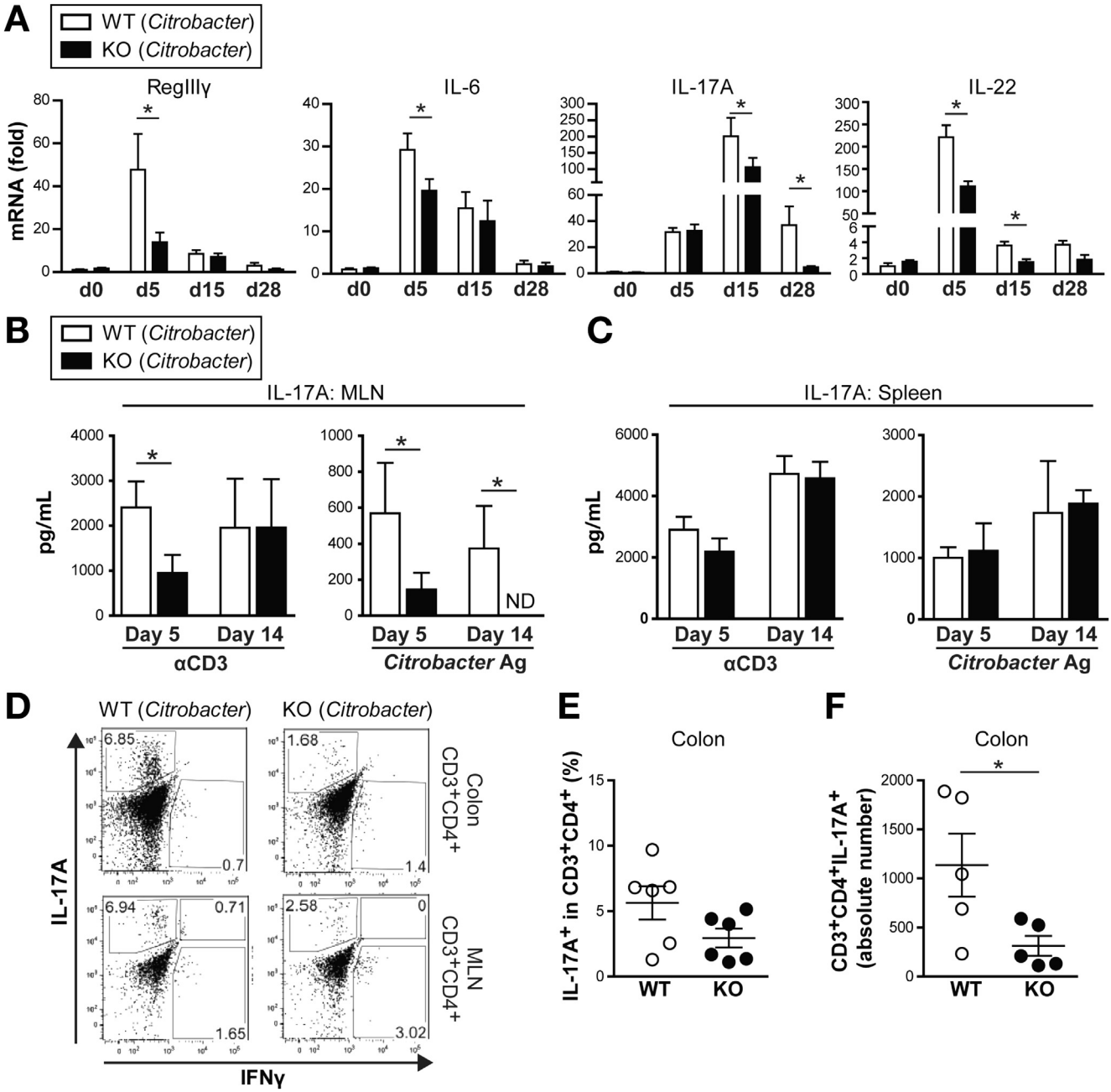


**Figure 4.** Card9 is required for Th17 and ILC responses in colon after *C rodentium* infection. (*A*) Cytokine expression in colon of wild-type (WT) and Card9-null (KO) mice after *C rodentium* infection, as quantified by qRT-PCR. Data are shown as fold changes relative to uninfected WT mice. (*B–C*) Secretion of IL-17A by (*B*) MLN and (*C*) spleen cells after *C rodentium* infection. Cells were stimulated with anti-CD3 or *C rodentium* antigen. ND, not detectable. (*D*) IL-17A and IFNγ intracellular staining of $CD3^+CD4^+$ T cells from colon LP lymphocytes (*top*) and MLN (*bottom*). Representative fluorescence-activated cell sorter plots are shown. (*E*) Proportion of $IL\text{-}17A^+$ cells among colon LP lymphocyte $CD3^+CD4^+$ T cells. (*F*) Number of $CD3^+CD4^+IL\text{-}17A^+$ cells in colon LP lymphocytes. Data are representative of at least 2 independent experiments (N = 5). Error bars represent SEM. $^*P < .05$.

microbiota of wild-type and Card9-null mice using 18S analysis (Figure 3*A*). Interestingly, the level of total fungi was 70% higher in the gut microbiota of Card9-null mice compared with wild-type (Figure 3*A*). Moreover, greater fungal translocation to the MLN, as measured by 18S qRT-PCR, and higher levels of systemic ASCA were detected in Card9-null mice 5 days after withdrawal of DSS (Figure 3*B* and *C*). These data suggest that the gastrointestinal immune system is less efficient in controlling fungi in Card9-null mice. To address whether this alteration in Card9-null mice accounts for enhanced susceptibility to inflammation, we administered the antifungal drug fluconazole before, during, and after DSS exposure. Efficient depletion of the fungi population in the small intestine and colon was validated using qRT-PCR (data not shown). As previously published,[17] wild-type mice lost less body weight in the absence of fungi. Similarly, fluconazole-treated Card9-null mice showed less

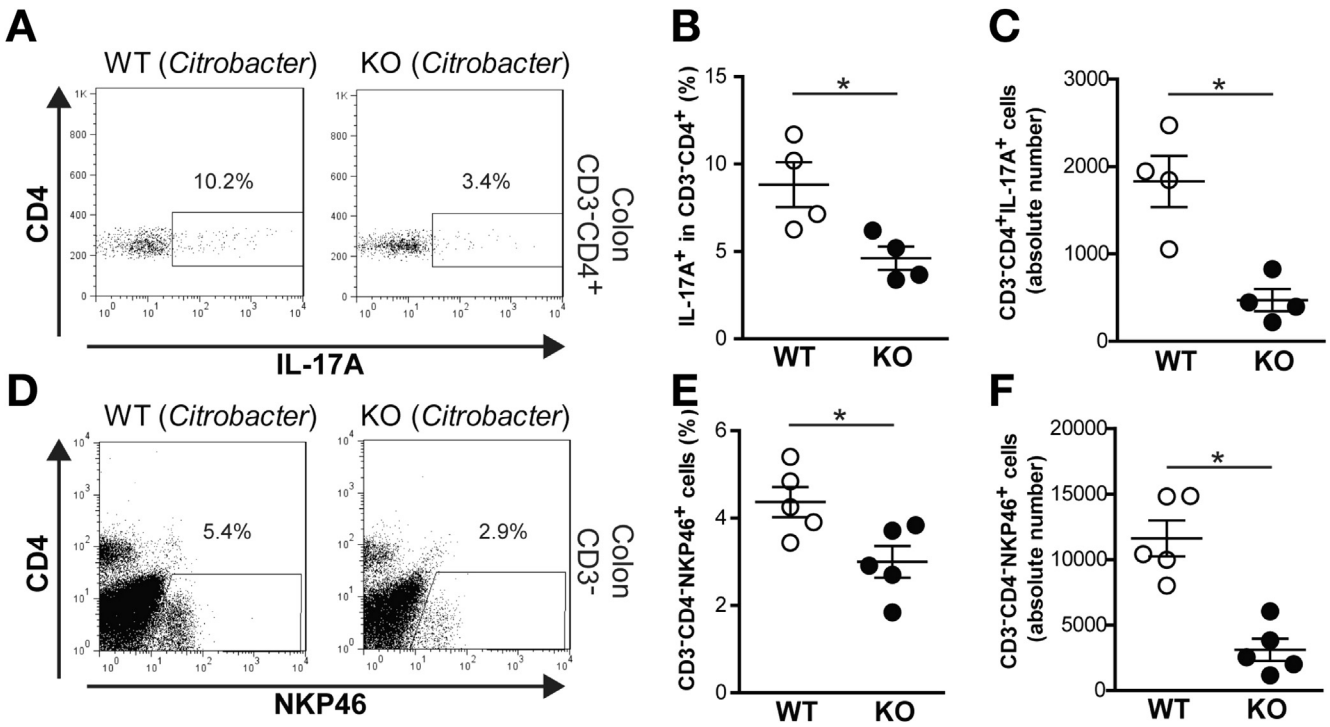


**Figure 5.** Card9 deficiency is associated with decreased ILCs in the gastrointestinal tract during *C rodentium* infection. (*A*) Representative fluorescence-activated cell sorter plots of $CD3^-CD4^+IL\text{-}17A^+$ ILCs in colon LP cells from wild-type (WT) and Card9-null (KO) mice. (*B*) Proportion and (*C*) number of $CD3^-CD4^+IL\text{-}17A^+$ ILCs in colon LP. (*D*) Representative fluorescence-activated cell sorter plots of $CD3^-CD4^-NKP46^+$ ILCs in colon LP cells. (*E*) Proportion and (*F*) number of $CD3^-CD4^-NKP46^+$ ILCs in colon LP. Data are representative of at least 2 independent experiments (N = 4–6). Error bars represent SEM. *$P < .05$.

body weight loss than their nontreated counterparts. However, the fluconazole-treated Card9-null mice showed greater weight loss than fluconazole-treated wild-type mice (Figure 3*D*). Consistent with our observations from mice treated only with DSS (Figure 2*B*), MLN T cells from fluconazole-treated Card9-null mice produced significantly lower amounts of IL-17A and IFNγ than wild-type mice (Figure 3*E*). Together, these observations suggest that fungal burden alone does not account for the differences we report.

### *Card9 Is Required to Mount an Appropriate Immune Response Toward* C Rodentium

The results acquired in 2 epithelial injury models suggest that Card9 is involved in Th17 responses, and we therefore next used the *C rodentium* colitis model in which IL-17A, IL-17F, and IL-22 are required for protection against infection.[22,25] *C rodentium* is a gram-negative attaching and effacing bacterial pathogen equivalent to the human enteropathogenic *Escherichia coli*,[26] which infects mouse colon and causes inflammation. We first assessed colonic RegIIIγ, IL-6, IL-17A, and IL-22 expression after *C rodentium* infection (Figure 4*A*). As previously reported,[25] IL-22, IL-6, and RegIIIγ were induced rapidly, with peak expression around day 5 after infection, whereas IL-17A induction was slower, reaching maximal levels 2 weeks after infection (Figure 4*A*). In Card9-null mice, the induction of RegIIIγ, IL-6, and Th17 cytokines was lower compared with wild-type mice, suggesting an impaired immune response to *C rodentium*.

We further investigated the immune response elicited by *C rodentium* by examining total and antigen-specific T-cell cytokine production in MLNs and spleen 5 and 14 days after infection. Isolated MLN lymphocytes were restimulated in vitro with *C rodentium* antigen or anti-CD3 antibody and, as anticipated, IL-17A production in response to both stimulations was significantly lower in Card9-null mice on day 5 (Figure 4*B*). However, 2 weeks after infection, the differences between wild-type and Card9-null IL-17A levels persisted only after antigen-specific stimulation (Figure 4*B*). No significant differences were observed in the spleen, suggesting that T-cell responses are not globally defective but are impaired specifically in cells involved in gut immunity (Figure 4*C*). Similar results were observed for IFNγ secretion (Supplementary Figure 4*A* and *B*).

We next isolated colonic LP cells to assess the frequency and number of Th17 cells in wild-type and Card9-null mice. As shown in Figure 4*D–F*, Card9-null mice had significantly fewer $CD3^+CD4^+IL\text{-}17A^+$ cells present during *C rodentium* infection. Given this phenotype in the *C rodentium* model, we revisited the DSS injury model and likewise observed significantly fewer $CD3^+CD4^+IL\text{-}17A^+$ cells in Card9-null mice in this model (Supplementary Figure 2*C* and *D*). Taken together, these data confirm that Card9 is required for Th17-mediated intestinal immune responses.

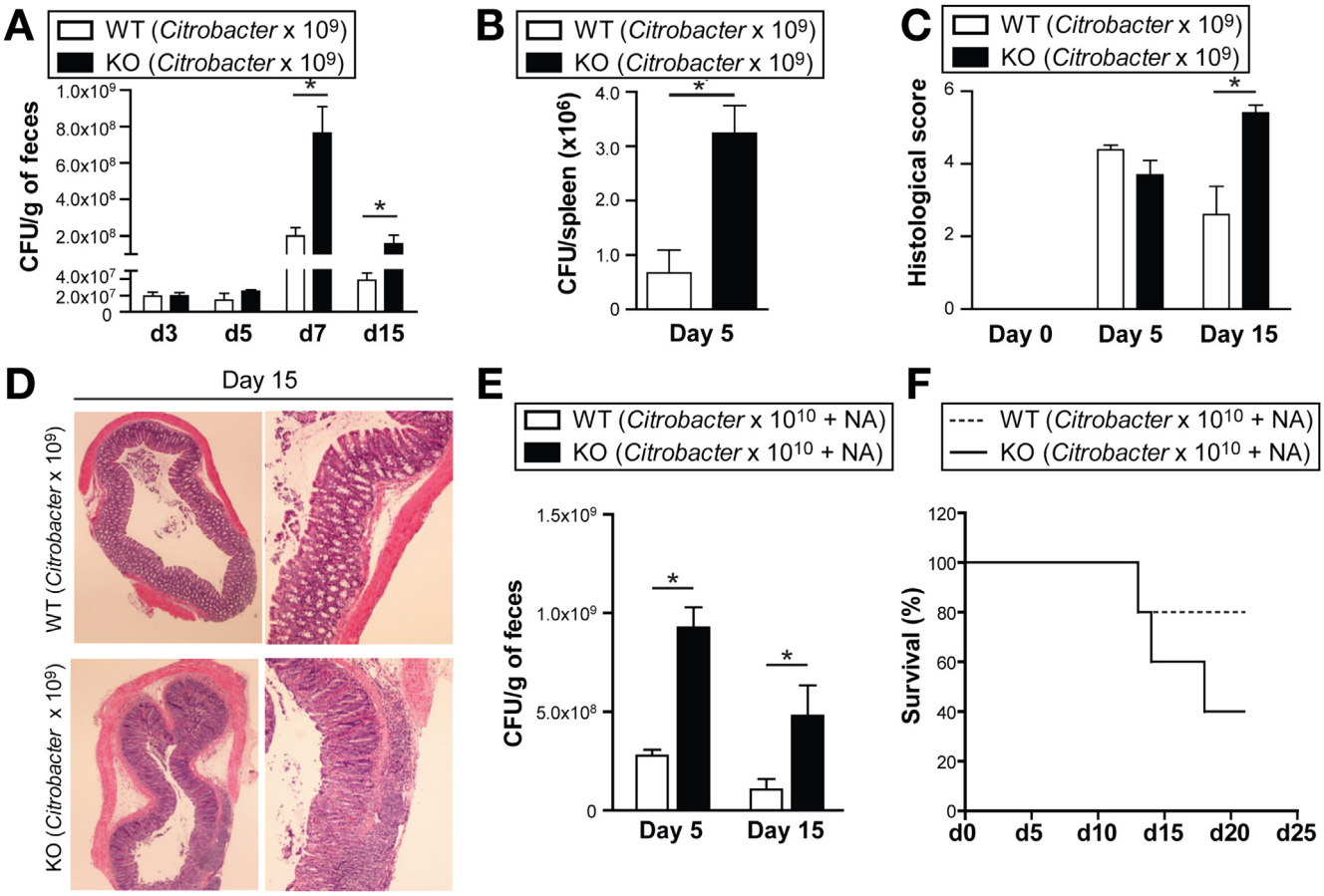


**Figure 6.** Card9 is required to control *C rodentium* infection. (*A*) *C rodentium* count in feces after infection in wild-type (WT) and Card9-null (KO). (*B*) *C rodentium* count in spleen 5 days after infection. (*C*) Colitis histology score at indicated time points after infection. (*D*) H&E staining of representative cross-sections of medial colon (magnification, 20×) on day 15 after infection. (*E*) *C rodentium* count in feces of mice pretreated with 100 μg nalidixic acid (NA) and infected with $10^{10}$ CFU *C rodentium*. (*F*) Survival curve of mice pretreated with 100 μg NA and infected with $10^{10}$ CFU *C rodentium*. Data are representative of at least 2 independent experiments (N = 5). Error bars represent SEM. *$P < .05$.



### *Card9 Deficiency Is Associated With Decreased ILCs in the Gastrointestinal Tract During* C Rodentium *Infection*

In addition to Th17 cells, ILCs also produce IL-17A and IL-22 in the gut, particularly during *C rodentium* infection.[27–31] Analysis of colon LP cells 5 days after *C rodentium* infection showed that Card9-null mice had a decreased frequency and number of $CD3^-CD4^+IL\text{-}17A^+$ and $CD3^-CD4^-NKP46^+$ ILC populations compared with wild-type mice (Figure 5*A*–*F*). These results suggest that Card9 is required not only for the development of Th17 cells, but also is important for the generation and/or recruitment of ILCs in the gastrointestinal tract during *C rodentium* infection.

### *Card9 Is Required to Control* C rodentium *Infection*

Given the observed defect in IL-17A and IL-22 pathways in Card9-null mice during *C rodentium*–induced colitis, we hypothesized that these mice would be unable to control bacterial propagation and therefore would be more susceptible to infection. As predicted, the levels of *C rodentium* present in the feces of Card9-null mice were higher than in wild-type mice 7 and 15 days after oral infection with *C rodentium* (Figure 6*A*), indicating impairment in bacterial clearance. Complementing these results, we observed increased *C rodentium* translocation to the spleen 5 days after infection in Card9-null mice compared with wild-type mice (Figure 6*B*). In addition, the severity of colitis, as assessed by histologic scoring, was higher in Card9-null mice 15 days after infection (Figure 6*C* and *D*). Despite increased colitis severity, no mortality was observed and all animals recovered within several weeks.

To better discriminate the altered phenotype in Card9-null mice, we used a modified protocol for *C rodentium* infection.[32] Mice were pretreated with nalidixic acid to disrupt the microbiota and infected with $1 \times 10^{10}$ CFU *C rodentium*, a dose 10-fold higher than in the earlier-described experiments. In addition to the expected higher levels of *C rodentium* in the feces of Card9-null mice (Figure 6*E*), the Card9-null mice showed an increased mortality rate compared with wild-type mice (Figure 6*F*), confirming heightened susceptibility to this bacterium.

## Discussion

CARD9 is a key adapter molecule that regulates responses to various microbes as well as responses to tissue injury associated with high levels of apoptosis.[33] Although the role of CARD9 in systemic immunity against fungi and other microbes has been explored,[1] its function in the gastrointestinal tract was unknown before this report. Here, we present evidence that Card9 is important in epithelial injury, ILC, and Th17 responses. Card9-null mice were more susceptible to DSS colitis than wild-type mice as a result of delayed recovery characterized by impaired colonic IFNγ, IL-6, IL-17A, IL-22, and Ccl20 expression. In addition, AMP expression was reduced in Card9-null mice, implicating a defect in the epithelial responses important for healing. By using the *C rodentium* colitis model, which requires IL-22, IL-17A, and IL-6 for protection,[22,25,32] we validated the findings observed in the DSS system. As predicted, Card9-null mice showed impaired expression of IL-6, IL-17A, IL-22, and RegIIIγ in the colon, and fewer Th17 cells and ILCs were detected in the colon LP during *C rodentium* infection. Based on the insight gained from these 2 models, we propose that Card9 mediates IL-17 and IL-22 signaling pathways, which subsequently regulate intestinal defense mechanisms.

Many pathways function in a coordinated manner to restore homeostasis after epithelial injury, and the data shown here suggest that Card9 may be a novel player in these restitutive processes. After epithelial damage, cytokines and chemokines are secreted to recruit immune cells to the site of injury, whereas necrotic and apoptotic cells release prostaglandin $E_2$ and other growth factors to induce cellular proliferation.[34] Wnt5a expression is known to regulate transforming growth factor-$\beta$ and is required for intestinal epithelial crypt generation, highlighting the diverse pathways necessary for epithelial restitution.[35] In addition, IL-22 also regulates mucosal wound healing,[20] and defects in this cytokine exacerbate DSS-induced colitis.[36] IL-22 aids in intestinal restitution by inducing expression of epithelial RegIIIγ; as expected, we show here that Card9-null mice express significantly lower levels of RegIIIγ compared with wild-type after recovery from DSS injury. Moreover, Card9-null mice displayed impaired healing after the introduction of epithelial micro-wounds using laser photodamage, highlighting an inherent defect in restitution. Thus, Card9 expression is required for reestablishing epithelial homeostasis after injury.

ILCs, a main source of IL-22 in both mice and human beings, continuously produce IL-22 to fortify the epithelial barrier.[37–39] Because IL-22 messenger RNA levels after acute DSS injury (day 7) were comparable in wild-type and Card9-null mice, but significantly reduced in Card9-null mice after recovery (day 12), we speculate that ILC recruitment and/or proliferation, rather than development, requires Card9 signaling, which will be the subject of future studies. Consistent with this hypothesis, we show that the reduced colonic IL-22 and IL-17 levels in Card9-null mice correlate with a decreased number of $CD3^-CD4^+IL17^+$ and $CD3^-CD4^+NKp46^+$ ILCs after epithelial injury. Expression of Ccl20, the ligand for the chemokine receptor Ccr6 that is secreted by myeloid cells to recruit Th17 and ILC populations to the site of injury, is also lower in Card9-null mice after recovery from DSS. Moreover, activated Card9-null macrophages secrete significantly less Ccl20 in response to bacterial ligands in vitro. Together, these data suggest that Card9 may control ILC recruitment to the injury site through induction of Ccl20 by myeloid cells. In addition to ILCs, we show lower absolute numbers of Th17 cells in Card9-null mice after epithelial injury, further suggesting that aberrant Ccl20-mediated recruitment of innate and adaptive immune cells may contribute to enhanced inflammation. Alternatively, Card9 may control ILC and Th17 expansion and function by inducing homeostatic cytokines such as IL-23, which we have shown to be lower in Card9-null mice after recovery from DSS-induced injury.

In addition to defective Th17 cell recruitment, T-cell differentiation also may be compromised in Card9-null mice. IL-6 is required for Th17 cell differentiation in mice,[40] and here we show lower levels of IL-6 in Card9-null mice during colitis, which is coincident with a decrease in colonic Th17 cells. Indeed, signals downstream of the Card9 receptors dectin-1 and dectin-2, as well as other pattern recognition receptors, have been shown to direct T-cell differentiation, depending on the receptors that are engaged.[41] Recent studies have shown that SFB can induce Th17 differentiation[24]; however, our data suggest that this mechanism is not skewing our results because both wild-type and Card9-null mice possess similar levels of these bacteria. Therefore, Card9 not only may regulate immune cell recruitment, but also may direct effector T-cell differentiation, both of which are critical during mucosal inflammation.

In addition to bacteria, an abundant and diverse fungal population exists in the gut[42] and CARD9 plays a major role in fungal sensing. Mice lacking dectin-1, a Card9-dependent receptor, show increased susceptibility to DSS colitis with an altered response to commensal fungi.[17] Similarly, we show here that in the absence of Card9, greater fungal colonization exists in the intestine, suggesting that this adaptor protein plays a role in controlling gut fungi. Consistent with this finding, Card9-null mice have higher systemic ASCA and fungal translocation after DSS injury. However, our experiments using antifungal administration suggest that the greater fungal burden does not solely account for the impaired Th17 and IL-22 responses we describe. Therefore, Card9 signaling regulates fungi and, in addition to other Card9-mediated processes, plays a role in intestinal homeostasis.

In conclusion, we have shown that Card9 orchestrates Th17- and ILC-mediated immune responses, which are important for restitution after epithelial injury. The mechanisms by which Card9 regulates these processes will be the subject of future studies.

## Supplementary Material

Note: To access the supplementary material accompanying this article, visit the online version of *Gastroenterology* at www.gastrojournal.org, and at http://dx.doi.org/10.1053/j.gastro.2013.05.047.

### References


1. Ruland J. CARD9 signaling in the innate immune response. Ann N Y Acad Sci 2008;1143:35–44.
2. Gross O, Gewies A, Finger K, et al. Card9 controls a non-TLR signalling pathway for innate anti-fungal immunity. Nature 2006; 442:651–656.
3. Hara H, Ishihara C, Takeuchi A, et al. The adaptor protein CARD9 is essential for the activation of myeloid cells through ITAM-associated and Toll-like receptors. Nat Immunol 2007;8:619–629.
4. **Glocker EO**, **Hennigs A**, Nabavi M, et al. A homozygous CARD9 mutation in a family with susceptibility to fungal infections. N Engl J Med 2009;361:1727–1735.
5. Gringhuis SI, Wevers BA, Kaptein TM, et al. Selective C-Rel activation via Malt1 controls anti-fungal T(H)-17 immunity by dectin-1 and dectin-2. PLoS Pathog 2011;7:e1001259.
6. LeibundGut-Landmann S, Gross O, Robinson MJ, et al. Syk- and CARD9-dependent coupling of innate immunity to the induction of T helper cells that produce interleukin 17. Nat Immunol 2007;8:630–638.
7. Schoenen H, Bodendorfer B, Hitchens K, et al. Cutting edge: mincle is essential for recognition and adjuvanticity of the mycobacterial cord factor and its synthetic analog trehalose-dibehenate. J Immunol 2010;184:2756–2760.
8. Hsu YM, Zhang Y, You Y, et al. The adaptor protein CARD9 is required for innate immune responses to intracellular pathogens. Nat Immunol 2007;8:198–205.
9. Goodridge HS, Shimada T, Wolf AJ, et al. Differential use of CARD9 by dectin-1 in macrophages and dendritic cells. J Immunol 2009; 182:1146–1154.
10. Hara H, Ishihara C, Takeuchi A, et al. Cell type-specific regulation of ITAM-mediated NF-kappaB activation by the adaptors, CARMA1 and CARD9. J Immunol 2008;181:918–930.
11. **Wu W**, **Hsu YM**, Bi L, et al. CARD9 facilitates microbe-elicited production of reactive oxygen species by regulating the LyGDI-Rac1 complex. Nat Immunol 2009;10:1208–1214.
12. **Poeck H**, **Bscheider M**, **Gross O**, et al. Recognition of RNA virus by RIG-I results in activation of CARD9 and inflammasome signaling for interleukin 1 beta production. Nat Immunol 2010;11:63–69.
13. Vallance BA, Deng W, Knodler LA, et al. Mice lacking T and B lymphocytes develop transient colitis and crypt hyperplasia yet suffer impaired bacterial clearance during Citrobacter rodentium infection. Infect Immun 2002;70:2070–2081.
14. Chen CC, Louie S, McCormick B, et al. Concurrent infection with an intestinal helminth parasite impairs host resistance to enteric Citrobacter rodentium and enhances Citrobacter-induced colitis in mice. Infect Immun 2005;73:5468–5481.
15. Kim P, Chung E, Yamashita H, et al. In vivo wide-area cellular imaging by side-view endomicroscopy. Nat Methods 2010;7:303–305.
16. **Kim JK**, **Lee WM**, **Kim P**, et al. Fabrication and operation of GRIN probes for in vivo fluorescence cellular imaging of internal organs in small animals. Nat Protoc 2012;7:1456–1469.
17. Iliev ID, Funari VA, Taylor KD, et al. Interactions between commensal fungi and the C-type lectin receptor Dectin-1 influence colitis. Science 2012;336:1314–1317.
18. **Grivennikov S**, **Karin E**, **Terzic J**, et al. IL-6 and Stat3 are required for survival of intestinal epithelial cells and development of colitis-associated cancer. Cancer Cell 2009;15:103–113.
19. Mashimo H, Wu DC, Podolsky DK, et al. Impaired defense of intestinal mucosa in mice lacking intestinal trefoil factor. Science 1996; 274:262–265.
20. **Pickert G**, **Neufert C**, Leppkes M, et al. STAT3 links IL-22 signaling in intestinal epithelial cells to mucosal wound healing. J Exp Med 2009;206:1465–1472.
21. Sonnenberg GF, Fouser LA, Artis D. Border patrol: regulation of immunity, inflammation and tissue homeostasis at barrier surfaces by IL-22. Nat Immunol 2011;12:383–390.
22. Ishigame H, Kakuta S, Nagai T, et al. Differential roles of interleukin-17A and -17F in host defense against mucoepithelial bacterial infection and allergic responses. Immunity 2009;30:108–119.
23. Gaboriau-Routhiau V, Rakotobe S, Lecuyer E, et al. The key role of segmented filamentous bacteria in the coordinated maturation of gut helper T cell responses. Immunity 2009;31:677–689.
24. **Ivanov II**, **Atarashi K**, Manel N, et al. Induction of intestinal Th17 cells by segmented filamentous bacteria. Cell 2009; 139:485–498.
25. Zheng Y, Valdez PA, Danilenko DM, et al. Interleukin-22 mediates early host defense against attaching and effacing bacterial pathogens. Nat Med 2008;14:282–289.
26. Schauer DB, Zabel BA, Pedraza IF, et al. Genetic and biochemical characterization of Citrobacter rodentium sp. nov. J Clin Microbiol 1995;33:2064–2068.
27. **Cella M**, **Fuchs A**, Vermi W, et al. A human natural killer cell subset provides an innate source of IL-22 for mucosal immunity. Nature 2009;457:722–725.
28. Sanos SL, Bui VL, Mortha A, et al. RORgammat and commensal microflora are required for the differentiation of mucosal interleukin 22-producing NKp46+ cells. Nat Immunol 2009;10:83–91.
29. Satoh-Takayama N, Vosshenrich CA, Lesjean-Pottier S, et al. Microbial flora drives interleukin 22 production in intestinal NKp46+ cells that provide innate mucosal immune defense. Immunity 2008; 29:958–970.
30. Sonnenberg GF, Monticelli LA, Elloso MM, et al. CD4(+) lymphoid tissue-inducer cells promote innate immunity in the gut. Immunity 2011;34:122–134.
31. Takatori H, Kanno Y, Watford WT, et al. Lymphoid tissue inducer-like cells are an innate source of IL-17 and IL-22. J Exp Med 2009;206:35–41.
32. **Geddes K**, **Rubino SJ**, Magalhaes JG, et al. Identification of an innate T helper type 17 response to intestinal bacterial pathogens. Nat Med 2011;17:837–844.
33. Hara H, Saito T. CARD9 versus CARMA1 in innate and adaptive immunity. Trends Immunol 2009;30:234–242.
34. **Arwert EN**, **Hoste E**, Watt FM. Epithelial stem cells, wound healing and cancer. Nat Rev Cancer 2012;12:170–180.
35. Miyoshi H, Ajima R, Luo CT, et al. Wnt5a potentiates TGF-beta signaling to promote colonic crypt regeneration after tissue injury. Science 2012;338:108–113.
36. Bettelli E, Oukka M, Kuchroo VK. T(H)-17 cells in the circle of immunity and autoimmunity. Nat Immunol 2007;8:345–350.
37. Colonna M. Interleukin-22-producing natural killer cells and lymphoid tissue inducer-like cells in mucosal immunity. Immunity 2009; 31:15–23.
38. Sonnenberg GF, Monticelli LA, Alenghat T, et al. Innate lymphoid cells promote anatomical containment of lymphoid-resident commensal bacteria. Science 2012;336:1321–1325.
39. Pearson C, Uhlig HH, Powrie F. Lymphoid microenvironments and innate lymphoid cells in the gut. Trends Immunol 2012; 33:289–296.
40. Sugimoto K, Ogawa A, Mizoguchi E, et al. IL-22 ameliorates intestinal inflammation in a mouse model of ulcerative colitis. J Clin Invest 2008;118:534–544.
41. Geijtenbeek TB, Gringhuis SI. Signalling through C-type lectin receptors: shaping immune responses. Nat Rev Immunol 2009;9:465–479.
42. Ott SJ, Kuhbacher T, Musfeldt M, et al. Fungi and inflammatory bowel diseases: alterations of composition and diversity. Scand J Gastroenterol 2008;43:831–841.


Author names in bold designate shared co-first authorship.

Received August 21, 2012. Accepted May 27, 2013.

*Reprint requests*

Address requests for reprints to: Ramnik Xavier, MD, PhD, Center for Computational and Integrative Biology, Massachusetts General Hospital, Richard B. Simches Research Center, 185 Cambridge Street, Boston, Massachusetts 02114. e-mail: xavier@molbio.mgh.harvard.edu; fax: (617) 643-3328.

*Conflicts of interest*

The authors disclose no conflicts.

*Funding*

Supported by grants from the French Society of Gastroenterology, the Bettencourt Schueller Foundation, the Ferring Fellowship, and the Arthur Sachs Scholarship (H.S.); The Netherlands Organization for Scientific Research (C.W.); by grants from the National Institutes of Health (DK083756, DK043351, DK086502, and DK060049), the Crohn's and Colitis Foundation of America, and The Leona M. and Harry B. Helmsley Charitable Trust (R.J.X.).

Editorial assistance was provided by Natalia Nedelsky, as supported by National Institutes of Health grant DK043351 (R.J.X.).

## Supplementary Materials and Methods

### *Animals*

Mice were maintained in specific-pathogen–free facilities at Massachusetts General Hospital. Card9-null mice on the C57/BL6j background (back-crossed 10 times) were provided by Takashi Saito (RIKEN Research Center for Allergy and Immunology, Yokohama, Japan) and have been described previously.[1] All mice were maintained on food and water ad libitum. Littermate and sex-matched mice were used at 7–9 weeks of age and co-housed for all experiments.

### *Histology*

Colon tissue was fixed in 10% buffered formalin and embedded in paraffin. Sections (5-$\mu$m) were stained with H&E. Tissues were scored blindly using established methods for both DSS and *C rodentium* colitis.[2,3] The results presented show the histologic evaluation of the mid-part of the colon.

### *qRT-PCR*

Proximal, medial, and distal colon tissues were harvested at the end of each course of colitis and stored in RNA*later* (Ambion, Austin, TX). RNA was extracted from homogenized tissues using the RNeasy Kit (Qiagen, Valencia, CA). RNA samples were reverse-transcribed using the iScript cDNA Synthesis kit (Bio-Rad Laboratories, Hercules, CA). By using the iQ SYBR Green Supermix (Bio-Rad) for quantitative PCR, messenger RNA levels were determined using the iCycler with the iQ5 Multicolor Real-Time PCR Detection System (Bio-Rad). Reaction conditions consisted of 40 cycles of PCR with 58°C or 59°C annealing temperature. The following primers were used: TNF-$\alpha$: forward: GACGTGGAACTGGCAGAAGAG; reverse: TTGGTGGTTTGTGAGTGTGAG; IFN$\gamma$: forward: ATGAACGCTACACACTGCATC; reverse: CCATCCTTTT GCCAGTTCCTC; IL-6: forward: GTAGCTATGGTACT CCAGAAGAC; reverse: ACGATGATGCACTTGCAGAA; IL-10: forward: AGAAGCATGGCCCAGAAATCA; reverse: GGCCTTGTAGACACCTTGGT; IL-17A: forward: TTTAA CTCCCTTGGCGCAAAA; reverse: CTTTCCCTCCGCAT TGACAC; IL-17F: forward: TGCTACTGTTGATGTTG GGAC; reverse: AATGCCCTGGTTTTGGTTGAA; IL-21: forward: CGCCTCCTGATTAGACTTCG; reverse: CAG GGTTTGATGGCTTGAGT; IL-22: forward: CATGCAG GAGGTGGTACCTT; reverse: CAGACGCAAGCATTTCT CAG; IL-23: forward: AGCGGGACATATGAATCTACTA AGAGA; reverse: GTCCTAGTAGGGAGGTGTGAAGTTG; IL-23R: forward: AGCAAAATCATCCCACGAAC; reverse: GCCACTTTGGGATCATCAGT CCL20; forward: GCCTC TCGTACATACAGACGC; reverse: CCAGTTCTGCTTTG GATCAGC; $\beta$-defensin 1: forward: AGGTGTTGGC ATTCTCACAAG; reverse: GCTTATCTGGTTTACAGGT TCCC MCP1; forward: CTGGATCGGAACCAAATGAG; reverse: AAGGCATCACAGTCCGAGTC; RegIII$\gamma$: forward: TCCTGTCCTCCATGATCAAAA; reverse: CATCCACCTC TGTTGGGTTCA.

The threshold cycle for each sample was determined for each gene and normalized to the threshold cycle value of the endogenous housekeeping gene glyceraldehyde-3-phosphate dehydrogenase. Data were calculated using a comparative threshold cycle method.

### *Lymphocyte Isolation and Measurement of Cytokine Production*

Lymphocyte suspensions were prepared from the MLN and spleen by pressing cells through a 70-$\mu$mol/L Falcon nylon cell strainer (BD Biosciences, San Jose, CA) in complete Dulbecco's modified Eagle medium (10% fetal calf serum, 10 mmol/L HEPES, 2 mmol/L L-glutamine, 100 U penicillin/mL, 100 $\mu$g streptomycin/mL, 50 $\mu$mol/L 2-mercaptoethanol, 0.1 mmol/L nonessential amino acids, and 1 mmol/L sodium pyruvate; Invitrogen Life Technologies, Carlsbad, CA). Cells ($5 \times 10^6$ cells/mL) were cultured in 24-well plates in the presence or absence of plate-bound anti-CD3 monoclonal antibody (10 $\mu$g/mL) or *C rodentium* Antigen (50 $\mu$g/mL), and culture supernatants were collected 72 hours later and stored at -20°C. IFN$\gamma$, IL-17A, IL-6, and TNF-$\alpha$ cytokines were assayed with an enzyme-linked immunosorbent assay using the following reagents: purified anti-mouse IL-17A (eBioscience, San Diego, CA), biotin anti-mouse IL-17A (eBioscience), purified anti-mouse IFN$\gamma$ (BD Biosciences, San Diego, CA), biotin anti-mouse IFN$\gamma$ (BD Biosciences), purified anti-mouse IL-6 (BD Biosciences), biotin anti-mouse IL-6 (BD Biosciences), purified anti-mouse TNF-$\alpha$ (BD Biosciences), biotin anti-mouse TNF-$\alpha$ (BD Biosciences), streptavidin-HRP (BD Biosciences), and OptEIA TMB Substrate (BD Biosciences).

### *Femtosecond Laser Injury to the Colon Epithelium*

We used a custom-built, 2-photon endomicroscopy system with a side-view probe.[4] After anesthetizing a mouse with an intraperitoneal injection of ketamine/xylazine solution (75 mg/kg ketamine and 15 mg/kg xylazine), we intravenously administered 2M-Da fluorescein isothiocyanate dextran (Sigma-Aldrich; 100 $\mu$L of 3% wt/vol). The mouse then was placed on a heated translation stage and fluorescent colonoscopy was performed as described previously.[5] After achieving stable positioning to the colonic epithelium, we increased the laser power to 200 milliwatts for 1 minute to induce photo-damage to the epithelium. Successful photo-damage was confirmed by observing the formation of intravascular clots and extravasation of the fluorescent dye.

### *Epithelial Barrier Function Assay*

At day 4 after femtosecond laser injury, we examined epithelial barrier function. The mouse was anesthetized by an intraperitoneal injection of ketamine/xylazine solution, the descending colon was washed by injecting 0.5 mL of warm PBS with a rubber-tipped syringe. Then, 0.5 mL of Evans Blue solution (4% wt/vol in

PBS) was instilled in the colon for 5 minutes and flushed with PBS to eliminate residual dye. The mouse was killed and the descending colon was collected for microscopic evaluation. The laser-injured region was found by residual green fluorescence from the leaked vascular dye. Bright-field images were taken in the control and injured regions to measure Evans Blue permeability.

### *SFB and Fungi Quantification in Fecal Microbiota*

Fecal DNA was extracted from 150 mg of stool using a DNA Stool Mini Kit (Qiagen). By using the iQ SYBR Green Supermix (Bio-Rad) for quantitative PCR, 16S or 18S ribosomal RNA gene levels were determined using the iCycler with the iQ5 Multicolor Real-Time PCR Detection System (Bio-Rad). Reaction conditions consisted of 40 cycles of PCR with a 59°C annealing temperature. The following primers were used: all bacteria: forward[6]: CGGTGAATACGTTCCCGG; reverse: TACGGCTACCTT GTTACGACTT; SFB: forward[7]: GACGCTGAGGCATGA GAGCAT; reverse: GACGGCACGGATTGTTATTCA 18S; forward[8]: ATTGGAGGGCAAGTCTGGTG; reverse: CCGA TCCCTAGTCGGCATAG.

The threshold cycle for each sample was determined for each gene and normalized to the $C_T$ value of the all-bacteria 16S ribosomal RNA gene. Data were calculated using the $2^{-\Delta\Delta C(T)}$ method.

### **C rodentium** *Antigen Preparation*

*C rodentium* antigen was prepared from an overnight culture of *C rodentium* in Luria broth. The bacterial culture was washed 3 times with PBS and sonicated on ice. The homogenate then was centrifuged (14,000 rpm) at 4°C for 30 minutes. Supernatants were collected and aliquots were stored at -20°C.

### *Lamina Propria Isolation*

Colonic and small intestine LP cells were isolated as previously described with slight modification. Briefly, colons and small intestine were harvested and placed in ice-cold Hank's balanced salt solution. After removal of residual mesenteric fat tissue, Peyer's patches were excised from small intestine, and the colon and small intestine were opened longitudinally. Tissues then were washed in ice-cold Hank's balanced salt solution and cut into 1-cm pieces. After 3 more washes in Hank's balanced salt solution, tissues were incubated twice in 20 mL of serum-free media with 5 mmol/L EDTA and 0.145 mg/mL dithiothreitol at 37°C at 250 rpm for 20 minutes. The pieces were washed 3 times with 10 mL of serum-free media with 2 mmol/L EDTA. After each incubation and wash, the epithelial cell layer containing the intra-epithelial lymphocytes was removed by intensive vortexing and passing through a 40-$\mu$m cell strainer, washed, and kept on ice until Percoll separation. Colon and small intestine pieces were next digested in serum-free media containing liberase (Roche Applied Science, Indianapolis, IN) and DNase I at 37°C at 250 rpm for 30 minutes. Cells were washed and passed through a 70-$\mu$m cell strainer. Cells were resuspended in 4.5 mL of 44% Percoll and placed on 2.3 mL of 67% Percoll. Percoll gradient separation was performed by centrifugation for 20 minutes at 600 $\times$ *g* at room temperature. Lymphoid fractions were collected at the interphase of the Percoll gradient, washed once, and resuspended in fluorescence-activated cell sorter buffer or culture medium. Cells were used immediately.

### *Flow Cytometry*

Cells were washed in PBS supplemented with 3% fetal bovine serum. For surface staining, cells were incubated with 2.4G2 Mouse Fc block in PBS supplemented with 3% fetal bovine serum (BD Pharmingen, San Diego, CA) for 20 minutes at 4°C. Cells were washed and stained with fluorescent-conjugated antibodies for 20 minutes at 4°C. The following antibodies were used for our analysis (BD Pharmingen): CD3–fluorescein isothiocyanate, CD4-PercP, IL-17A–allophycocyanin, and IFN$\gamma$-phycoerythrin. Fluorescently labeled LP cells were acquired on a FACSCalibur flow cytometer (BD Biosciences) and analyzed using FlowJo Analysis Software (Tree Star, Inc, Ashland, OR). For intracellular cytokine staining, immediately after isolation the cells were incubated for 5 hours at 37°C with 50 ng/mL phorbol myristate acetate (Sigma-Aldrich), 1 $\mu$mol/L ionomycin (Sigma-Aldrich), and 1 $\mu$L/mL GolgiPlug (BD Biosciences). Surface staining was performed followed by intracellular staining using the BD Cytofix/Cytoperm Kit (BD Biosciences).

### *Ethical Approval*

All animal studies were conducted under protocols approved by the Subcommittee on Research Animal Care at Massachusetts General Hospital, which serves as the Institutional Animal Care and Use Committee as required by Public Health Service policies on the Humane Care and Use of Laboratory Animals.

## Supplementary References


1. Hara H, Ishihara C, Takeuchi A, et al. The adaptor protein CARD9 is essential for the activation of myeloid cells through ITAM-associated and Toll-like receptors. Nat Immunol 2007; 8:619–629.
2. Chen CC, Louie S, McCormick B, et al. Concurrent infection with an intestinal helminth parasite impairs host resistance to enteric Citrobacter rodentium and enhances Citrobacter-induced colitis in mice. Infect Immun 2005;73:5468–5481.
3. Dieleman LA, Palmen MJ, Akol H, et al. Chronic experimental colitis induced by dextran sulphate sodium (DSS) is characterized by Th1 and Th2 cytokines. Clin Exp Immunol 1998;114:385–391.
4. Kim P, Chung E, Yamashita H, et al. In vivo wide-area cellular imaging by side-view endomicroscopy. Nat Methods 2010; 7:303–305.
5. **Kim JK**, **Lee WM**, **Kim P**, et al. Fabrication and operation of GRIN probes for in vivo fluorescence cellular imaging of internal organs in small animals. Nat Protoc 2012;7:1456–1469.
6. **Sokol H**, **Pigneur B**, Watterlot L, et al. Faecalibacterium prausnitzii is an anti-inflammatory commensal bacterium identified by gut microbiota analysis of Crohn disease patients. Proc Natl Acad Sci U S A 2008;105:16731–16736.
7. **Ivanov II**, **Atarashi K**, Manel N, et al. Induction of intestinal Th17 cells by segmented filamentous bacteria. Cell 2009;139:485–498.
8. Loeffler J, Hebart H, Cox P, et al. Nucleic acid sequence-based amplification of Aspergillus RNA in blood samples. J Clin Microbiol 2001;39:1626–1629.


Author names in bold designate shared co-authorship.